



Research article

Synthesis and characterization of bovine serum albumin-coated copper sulfide nanoparticles as curcumin nanocarriers

Ali Mohammadi^{a,b}, Hossein Danafar^{a,b,*}^a Student Research Center, Zanjan University of Medical Sciences, Zanjan, Iran^b Zanjan Pharmaceutical Nanotechnology Research Center, Zanjan University of Medical Sciences, Zanjan, Iran

ARTICLE INFO

Keywords:

Nanoparticles
Cytotoxicity
Albumin
Copper
Curcumin
Drug delivery

ABSTRACT

Cancer is among the most common causes of death in the world that affects a large number of people every year. Curcumin is one of the natural anticancer therapeutics with little or no negative effects. However, due to its hydrophobic nature, poor bioavailability, limited gastrointestinal uptake, and fast metabolism, its therapeutic applications are constrained. Therefore, the Bovine Serum Albumin-Coated Copper Sulfide nanoparticles (CuS@BSA) for curcumin (CUR) drug delivery were synthesized and characterized, and then curcumin release from the nanosystem. Hemotoxicity, and cytotoxicity was investigated. This study involved the one-step synthesis of CuS@BSA nanoparticles first, followed by the addition of CUR. Then the synthesized nanoparticles were characterized employing Scanning Transient Electron Microscopy (STEM), Ultraviolet-visible spectroscopy (UV-vis) and Fourier-transform infrared spectroscopy (FT-IR) techniques. The Size and surface charge (zeta potential) of synthesized nanoparticles were determined by Dynamic Light Scattering (DLS) to be 120 nm and -13 eV, respectively. The results showed that the CUR loading was around 15% and also the release pattern of CUR was dependent on pH and increased in an acidic environment. The results of the hemolysis assay showed that the synthesized nanoparticles are not hemotoxic. The investigation of the cytotoxic effects of synthesized nanoparticles on cancer cells demonstrated that CuS@BSA nanoparticles did not exhibit any toxicity and therefore are an appropriate candidate for drug delivery.

1. Introduction

Despite current medical developments, disease and mortality rates have not significantly changed from a decade ago. Conventional anti-cancer drugs provide little therapeutic effects, are costly and come with serious side effects [1]. Therefore, it is necessary to identify drug agents that do not have these disadvantages. Emerging natural compounds are effective agents for the treatment of malignant diseases. Extracts of some medicinal plants or phytochemicals have been reported to have anti-cancer activity at different stages of tumor growth [2]. About 60% of the chemotherapeutic agents used to treat cancer are derived from natural compounds, the main source of which is medicinal herbs [3]. One of these natural compounds is curcumin (CUR) (1,7-bis(4-hydroxy-3-methoxyphenyl)-1,6-heptadiene-3,5-dione) [4] that is the major component of turmeric [5]. CUR is gaining popularity in recent years as owing to its multifaceted roles such as antiseptic [6], anti-inflammatory [7,8], antioxidant activity [9], anti-osteoarthritis [10],

* Corresponding author. Department of Medicinal Chemistry School of Pharmacy Zanjan University of Medical Sciences Postal Code 45139-56184 Zanjan, Iran.

E-mail address: danafar@zums.ac.ir (H. Danafar).

<https://doi.org/10.1016/j.heliyon.2023.e13740>

Received 20 November 2022; Received in revised form 4 February 2023; Accepted 9 February 2023

Available online 14 February 2023

2405-8440/© 2023 Published by Elsevier Ltd.

This is an open access article under the CC BY-NC-ND license

(<http://creativecommons.org/licenses/by-nc-nd/4.0/>).

protection of the heart [11], protection of liver [12] Chemistry Prevention and anti-cancer [13–15] is nicknamed ‘next-generation multipurpose drug. CUR potentially act on cellular and molecular targets such as Nuclear factor κ -light-chain-enhancer of activate B cells (NF- κ B), Phosphatase and tensin homolog (PTEN), mitogen-activated protein kinases (MAPK), Protein kinase B (Akt), and microRNA exhibit their therapeutic properties [16]. It has been demonstrated that CUR inhibits the growth, development, and metastasis of a variety of cancers. However, CUR rapidly degrades at physiological pH and is very weakly soluble in an aqueous solution (20 g/mL) [17]. Due to its poor bioavailability at the tumor site and lower pharmacokinetics, it has a constrained place in the treatment of cancer [18]. New drug delivery systems are used to improve pharmacokinetics and hydrophilic properties. In recent years, significant progress has been achieved in the development of carrier-assisted drug delivery systems (DDSs) for the treatment of cancer [19]. DDSs are really effective and few of them have undergone clinical trials [20]. The drug delivery system based on metal nanoparticles are part of the DDSs system and due to Nano architectures facilitates the selective accumulation in tumors due to the EPR effect. Copper nanoparticles have attracted the most interest among the various metal nanoparticles due to their low cost, extensive range of physiochemical properties, and high level of chemical activity [21,22]. Copper nanoparticles and their derivatives have been studied by many researchers today and their effects as radiation sensitizers in radiation therapy and their effects as photothermal therapy agents are being investigated [23,24]. As copper nanoparticles enter the systemic circulatory system, they interact with a variety of biomolecules, notably proteins, and this interaction is crucial to the pharmacokinetics (absorption, distribution, metabolism, and excretion) of nanoparticles [25,26]. The most abundant protein in plasma is albumin, which has recently received particular interest in the research of cancer treatment. BSA was used in this study due to its structural similarity with human serum albumin (HSA) as well as low cost and easy accessibility [27–29]. Coating of copper nanoparticles with BSA results in good surface functionality, stability, and long blood circulation. Finally, in this project, we decided to synthesize the CuS@BSA nanosystem for CUR delivery and investigate hematotoxicity as well as cell viability of the synthesized Nano system.

2. Materials and methods

2.1. Materials

All chemicals employed in this work were obtained from Sigma-Aldrich (St. Louis, USA) and Merck (Kenilworth, USA).

2.1.1. Synthesis of CuS@BSA

500 mg of BSA was dissolved in 15 mL of water for the synthesis of CuS@BSA nanoparticles, and 2 mL of CuNO₃ (0.2 M) was added while stirring the mixture with a magnetic stirrer. Then 2 mL of NaOH (1 M) was added and finally, 4 mL of thiourea (0.2 M) was added to the reaction mixture. The resulting mixture was then heated to 90 °C for 30 min, at which point the color became dark green, indicating the formation of the CuS@BSA nanoparticle. Finally, the resulting CuS@BSA nanoparticles were purified by dialysis.

2.1.2. Loading of curcumin in CuS@BSA nanoparticles

CuS@BSA-CUR nanoparticles were synthesized by dissolving 5 mg of CUR in 1.5 mL of DMSO. Under a magnetic stirrer, the prepared curcumin solution was added dropwise to the 10 mL of CuS@BSA nanoparticles (2 mg/mL) solution. After being stirred for 24 h at room temperature, CuS@BSA-CUR was finally centrifuged for purification.

2.2. Characterization

2.2.1. Morphology and size determination

STEM (Zeiss Gemini 500, Germany) was used for determining the shape and size of the synthesized nanoparticles.

2.2.2. Fourier-transform infrared spectroscopy (FTIR) analysis

FTIR was used to the determination of functional groups of the nanoparticles (Bruker, Tensor 27, USA). For this purpose, a small amount of the substance to be tested is mixed with potassium bromide and during the tableting process, the substance is prepared for analysis.

2.2.3. Ultraviolet–visible spectroscopy analysis

Nanoparticles were optically analyzed utilizing the UV–vis spectrum with Analyticgen SPECORD 210 PLUS model from Germany in the 200–600 nm range.

2.2.4. Dynamic Light Scattering (DLS) analysis

DLS (Malvern Instruments, Worcestershire, U.K., ZEN 3600 model Nano ZS) was used to determine the hydrodynamic size distribution and surface charge.

2.2.5. Loading efficiency determination

A spectrophotometric study was performed at 420 nm to measure the loaded CUR. First, 1 mg of CuS@BSA-CUR to the 2 mL of ethanol was dispersed. Vials were incubated for 30 min at 37 °C. Following centrifugation at 13,000 rpm, a UV–vis spectrophotometer was used to measure the CUR, and the percentage of loaded CUR was then determined as follows:

$$\text{Drug Loading (\%)} = \frac{\text{weight of drug in nanoparticles}}{\text{weight of drug loaded nanoparticles}} \times 100$$

2.2.6. Drug release study

Through the application of the dialysis method including both neutral (pH 7.2) and acidic (pH = 4.8) environments, the release pattern of CUR from the synthesized nanoparticles were investigated. An amount of 5 mg of CuS@BSA-CUR was dispersed in a 2 mL PBS: ethanol mixture poured into a dialysis bag, and then immersed in 35 mL of PBS: ethanol. The vials were then gently shaken while being incubated at 37 °C. A UV-Vis spectrophotometer was used to measure absorption at 420 nm wavelength in order to quantify CUR released. This assay three times was repeated.

2.2.7. Hemolysis assay

A hemolysis test is performed to check the biological compatibility of nanoparticles. Human blood is taken, the red blood cells are separated, and then the red blood cells are mixed with a solution containing samples with different concentrations. The mixture was shaken for 4 h at a temperature of 37° Celsius in a shaker incubator. Deionized water was used as a positive control in this assay and PBS solution as the negative control. Then the mixture is centrifuged for 15 min at a speed of 13,000 rpm and absorbance is read at 540 nm. The following formula determined the percentage of hemolysis:

$$\text{Hemolysis(\%)} = \frac{A_{\text{sample}} - A_{\text{negative}}}{A_{\text{positive}} - A_{\text{negative}}} \times 100$$

2.3. Cytotoxic effects on cancer cells

Human breast cancer MDA-MB-231 cells were cultured in the DMEM medium supplemented with 10% FBS and 1% penicillin/streptomycin at 37 °C. MDA-MB-231 cells were seeded in a 96-well plate at a density of 1×10^5 cells per well. After 24 h, the culture media was discarded, and the cells were subsequently treated with various doses of CuS@BSA-CUR (100 μ L) for 72 h. The incubation medium was then replaced with a fresh medium containing 20 μ L of MTT solution (2.5 mg/mL) and incubated for an additional 4 h. Dimethyl sulfoxide (DMSO) in the amount of 100 μ L was then added to each well in order to dissolve the violet formazan crystals that had formed. The absorbance of the dissolved formazan was measured at 570 nm using a microplate reader (Bio-Tek, USA) after shaking for 1 min.

3. Result and discussion

3.1. Fourier-transform infrared spectroscopy analysis

FTIR technique was used to evaluate the success of the synthesis. The characteristic CUR peaks, that correspond to the hydroxyl and carbonyl groups, were found in the range of 3437 cm^{-1} and 1628 cm^{-1} (C=O). The CuS@BSA characteristic peaks were found in the range of 3431 cm^{-1} , which corresponds to the N-H group of BSA. The interfacial bonding between CUR and CuS@BSA is responsible for the carbonyl group's (C = O) shift in the CuS@BSA-CUR structure relative to CuS@BSA towards the lower wavenumber (Fig. 1).

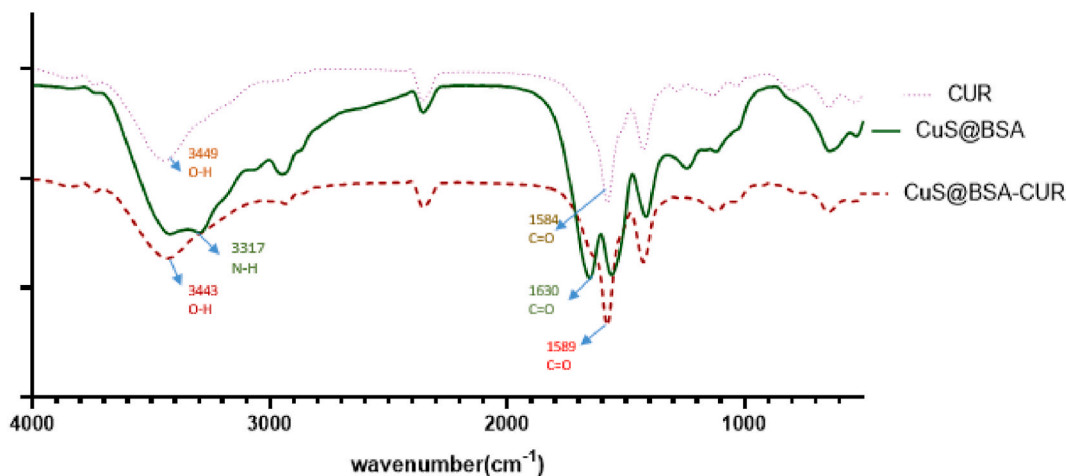


Fig. 1. Characterization technique using FT-IR. FT-IR spectra of free CUR, fabricated CuS@BSA and final nanoformulation of CuS@BSA-CUR

3.2. Ultraviolet–visible spectroscopy spectrophotometry analysis

The loading of CUR was confirmed using UV–Vis absorption spectra. As according to Fig. 2, the distinctive absorption peak in the CUR UV–Vis spectra is located at 420 nm and is related to the π – π^* transition. The interaction and loading of CUR into BSA nanoparticles were confirmed by the UV–Vis spectra of CuS@BSA-CUR, which exhibits the corresponding peak of CUR with a minor shift of 377 nm (Fig. 2).

3.3. Dynamic Light Scattering and Scanning Transient Electron Microscopy analysis

STEM and DLS analyses were used to determine the size, morphology, and zeta potential of CuS@BSA-CUR nanoparticles. The results clearly demonstrated that the NPs are spherical with a size range of 76.54 nm (Fig. 3).

3.4. Determination of drug loading and release study

Based on the previously mentioned CUR loading calculation method, the CUR loading value was calculated as 15%. Since curcumin release was pH-dependent, no significant initial release of curcumin from the synthesized nanoparticles were observed at pH 7.4 and the release value was 12%. By decreasing the pH to 4.8, the release rate reached 74%. This might be the result of curcumin being physically loaded into CuS@BSA. Therefore, to achieve a variety of therapeutic targets, our CuS@BSA could be considered a highly appealing time-controlled drug delivery nanocarrier for hydrophobic drugs (Fig. 4).

3.5. Hemolysis assay

A hemolytic rate of less than 5% was observed for all tested samples following 4 h of blood incubation with nanoparticles, as shown in Fig. 5. In accordance with ISO/TR 7406, samples are regarded as non-hemolytic when their hemolytic rate is less than 5% (the critical safe hemolytic ratio for biological materials). CuS@BSA-CUR nanoparticles have good compatibility and can be used as a candidate for intravenous injection.

3.6. Cytotoxic effects on cancer cells

The results of the MTT assay using CuS@BSA-CUR, CuS@BSA, and CUR on MDA-MB-231 cells revealed that increasing the concentration of CuS@BSA up to 72 $\mu\text{g}/\text{mL}$ seemed to have no cytotoxicity effect (Fig. 6). However, it was revealed that cell viability decreases as the concentration of CuS@BSA-CUR and CUR increase; at concentrations of 72 and 10.8 $\mu\text{g}/\text{mL}$, the cell viability decreases by 40 and 32%, respectively. According to the obtained results, it can be acknowledged that CuS@BSA is a non-toxic system and a suitable candidate for drug delivery.

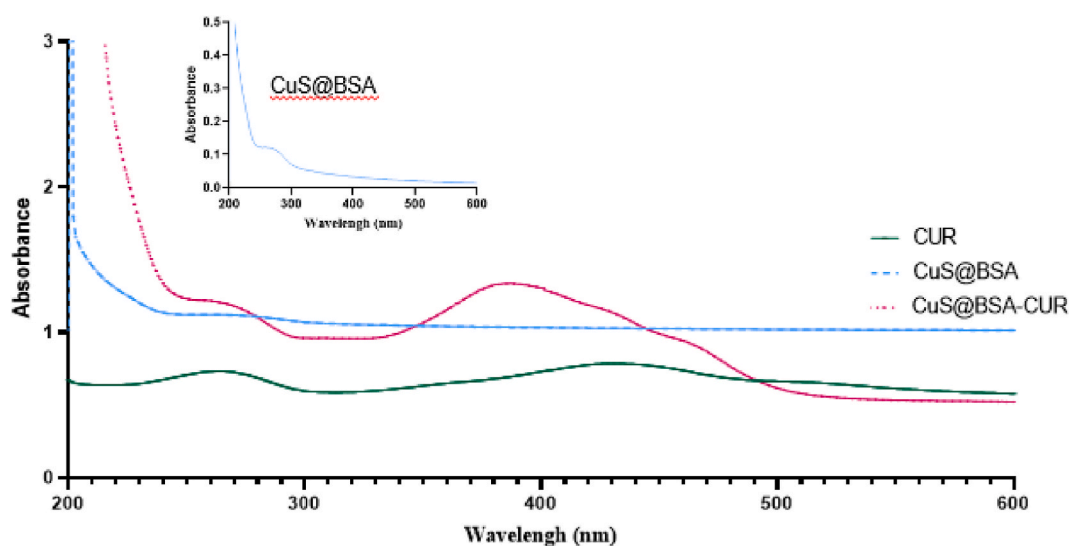


Fig. 2. Characterization of synthesized nanomaterials via UV–vis technique. The UV–vis absorption spectrum of CUR, CuS@BSA, and CuS@BSA-CUR within range of 200–600 nm.

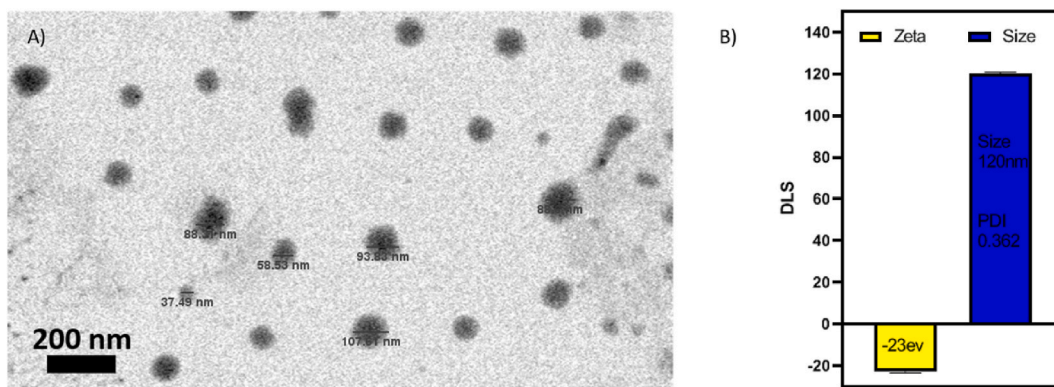


Fig. 3. A) Morphological analysis of nanoparticle's surface via STEM, B) Particle size and zeta potential measurement of CuS@BSA-CUR using DLS.

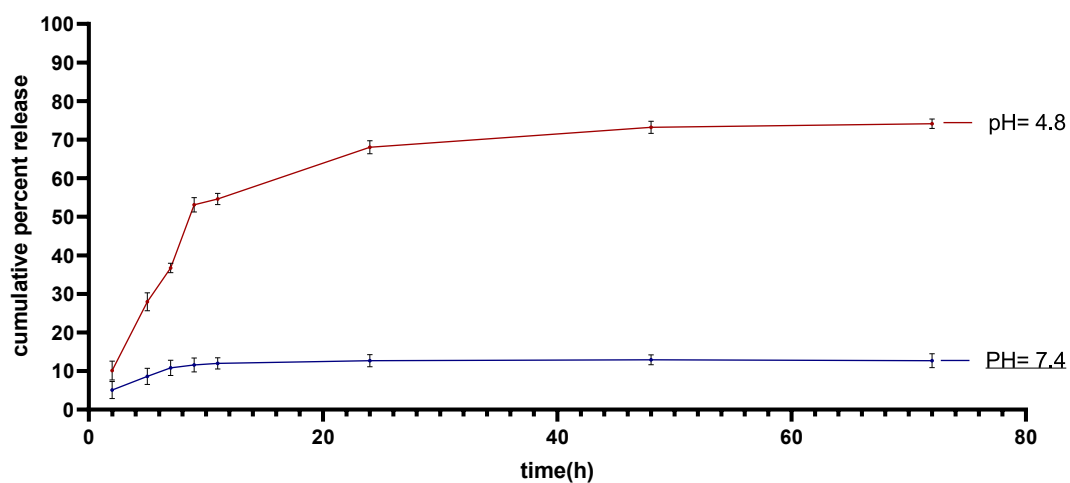


Fig. 4. Drug release profile study of CuS@BSA-CUR at normal physiological pH of 7.4 and acidic condition. The image showing the release profiles of CUR.

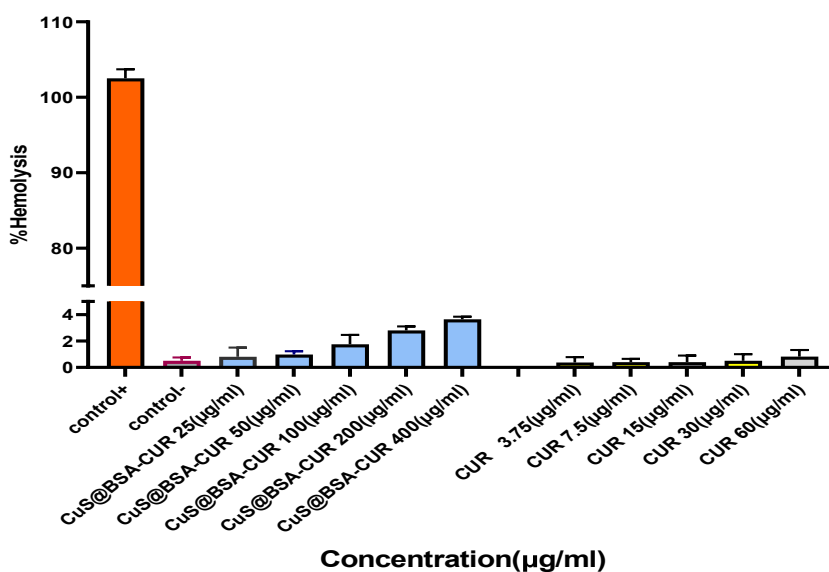


Fig. 5. *In vitro* hemolysis assay of Free CUR, CuS@BSA, and developed CuS@BSA-CUR over a wide range of concentrations.

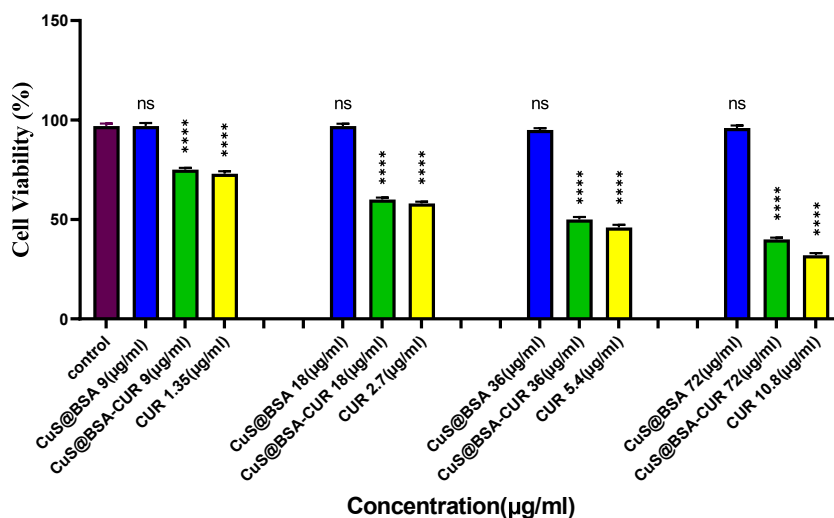


Fig. 6. Cell viability assay (MTT assay) of CUR, CuS@BSA, and developed CuS@BSA-CUR at concentration of 9, 18, 36 and 72 µg/mL and its equivalent curcumin. Statistically significance: * $p < 0.05$, ** $p < 0.01$, *** $p < 0.001$.

4. Conclusion

In short, CuS@BSA nanoparticles were successfully prepared by an easy method, and in the next step, the nanoparticles were loaded with curcumin. The synthesized nanoparticles were characterized by UV-vis, FT-IR and STEM techniques. The release results showed that the release of curcumin from the synthesized nanoparticles were sensitive to pH and showed 74% release in an acidic environment within 72 h. According to the Hemolysis assay, the synthesized nanoparticles are safe in terms of hematological toxicity. The results revealed that CuS@BSA had no inhibitory effects on cancer cells and that there was no statistically significant difference between the CuS@BSA-treated cells and the control group. Nevertheless, CuS@BSA-CUR nanoparticles showed a significant inhibitory effect on cancer cells. Also, cell viability data showed that CuS@BSA-CUR and curcumin showed almost similar effects, which can be attributed to the amount of free curcumin in the cell, according to the release rate of curcumin from the synthetic nanosystem.

Author contribution statement

Hossein Danafar: Conceived and designed the experiments; Analyzed and interpreted the data; Contributed reagents, materials, analysis tools or data.

Ali Mohammadi: Wrote the paper; Performed the experiments; Analyzed and interpreted the data.

Funding statement

This research did not receive any specific grant from funding agencies in the public, commercial, or not-for-profit sectors.

Data availability statement

No data was used for the research described in the article.

Declaration of interest's statement

The authors declare no conflict of interest.

Acknowledgments

This work was supported by the Deputy of Research of Zanjan University of Medical Sciences (grant no. A-12-430-40, ethical code: IR. ZUMS.REC.1398.457).

References

- [1] M.K. Shanmugam, et al., The multifaceted role of curcumin in cancer prevention and treatment, *Molecules* 20 (2) (2015) 2728–2769.
- [2] E. Solowey, et al., Evaluating medicinal plants for anticancer activity, *Sci. World J.* 2014 (2014).
- [3] G.M. Cragg, D.J. Newman, Nature: a vital source of leads for anticancer drug development, *Phytochemistry Rev.* 8 (2) (2009) 313–331.

- [4] M.M. Yallapu, M. Jaggi, S.C. Chauhan, β -Cyclodextrin-curcumin self-assembly enhances curcumin delivery in prostate cancer cells, *Colloids Surf. B Biointerfaces* 79 (1) (2010) 113–125.
- [5] E. Willenbacher, et al., Curcumin: new insights into an ancient ingredient against cancer, *Int. J. Mol. Sci.* 20 (8) (2019) 1808.
- [6] M.M.-Y. Chan, N.S. Adapala, D. Fong, Curcumin overcomes the inhibitory effect of nitric oxide on Leishmania, *Parasitol. Res.* 96 (1) (2005) 49–56.
- [7] I. Brouet, H. Ohshima, Curcumin, an anti-tumor promoter and anti-inflammatory agent, inhibits induction of nitric oxide synthase in activated macrophages, *Biochem. Biophys. Res. Commun.* 206 (2) (1995) 533–540.
- [8] M. Dikshit, et al., Prevention of ischaemia-induced biochemical changes by curcumin & quinidine in the cat heart, *Indian J. Med. Res.* 101 (1995) 31–35.
- [9] M. Rao, Nitric oxide scavenging by curcuminoids, *J. Pharm. Pharmacol.* 49 (1) (1997) 105–107.
- [10] S. Dcodhar, R. Sethi, R. Srimal, Preliminary study on antirheumatic activity of curcumin (diferuloyl methane), *Indian J. Med. Res.* 138 (1) (2013).
- [11] N. Venkatesan, Curcumin attenuation of acute adriamycin myocardial toxicity in rats, *Br. J. Pharmacol.* 124 (3) (1998) 425–427.
- [12] Y. Kiso, et al., Antihepatotoxic principles of *Curcuma longa* rhizomes, *Planta Med.* 49 (11) (1983) 185–187.
- [13] A. Chen, J. Xu, A. Johnson, Curcumin inhibits human colon cancer cell growth by suppressing gene expression of epidermal growth factor receptor through reducing the activity of the transcription factor Egr-1, *Oncogene* 25 (2) (2006) 278–287.
- [14] J. Chen, et al., Curcumin protects PC12 cells against 1-methyl-4-phenylpyridinium ion-induced apoptosis by bcl-2-mitochondria-ROS-iNOS pathway, *Apoptosis* 11 (6) (2006) 943–953.
- [15] C.S. Divya, M.R. Pillai, Antitumor action of curcumin in human papillomavirus associated cells involves downregulation of viral oncogenes, prevention of NFkB and AP-1 translocation, and modulation of apoptosis, *Mol. Carcinog.: Publ. Cooperat. Univ. Texas MD Anderson Cancer Center* 45 (5) (2006) 320–332.
- [16] H. Mirzaei, et al., Phytosomal curcumin: a review of pharmacokinetic, experimental and clinical studies, *Biomed. Pharmacother.* 85 (2017) 102–112.
- [17] Y.-J. Wang, et al., Stability of curcumin in buffer solutions and characterization of its degradation products, *J. Pharmaceut. Biomed. Anal.* 15 (12) (1997) 1867–1876.
- [18] P. Anand, et al., Bioavailability of curcumin: problems and promises, *Mol. Pharm.* 4 (6) (2007) 807–818.
- [19] S.-Y. Qin, et al., Drug self-delivery systems for cancer therapy, *Biomaterials* 112 (2017) 234–247.
- [20] N. Kamaly, et al., Targeted polymeric therapeutic nanoparticles: design, development and clinical translation, *Chem. Soc. Rev.* 41 (7) (2012) 2971–3010.
- [21] Y. Wen, et al., Synthesis of Cu nanoparticles for large-scale preparation, *Mater. Sci. Eng., B* 177 (8) (2012) 619–624.
- [22] Q.-m. Liu, et al., Preparation of Cu nanoparticles with NaBH₄ by aqueous reduction method, *Trans. Nonferrous Metals Soc. China* 22 (1) (2012) 117–123.
- [23] M. Zhou, et al., Single agent nanoparticle for radiotherapy and radio-photothermal therapy in anaplastic thyroid cancer, *Biomaterials* 57 (2015) 41–49.
- [24] Q. Chen, et al., Clearable theranostic platform with a pH-independent chemodynamic therapy enhancement strategy for synergetic photothermal tumor therapy, *ACS Appl. Mater. Interfaces* 11 (20) (2019) 18133–18144.
- [25] S. Sugio, et al., Crystal structure of human serum albumin at 2.5 Å resolution, *Protein Eng.* 12 (6) (1999) 439–446.
- [26] J. Flarakos, K.L. Morand, P. Vouros, High-throughput solution-based medicinal library screening against human serum albumin, *Anal. Chem.* 77 (5) (2005) 1345–1353.
- [27] T. Peters Jr., *All about Albumin: Biochemistry, Genetics, and Medical Applications*, 1995 (Academic press).
- [28] N.M. Urquiza, et al., Antioxidant activity of methimazole–copper (II) bioactive species and spectroscopic investigations on the mechanism of its interaction with Bovine Serum Albumin, *Polyhedron* 31 (1) (2012) 530–538.
- [29] Y. Xiang, F. Wu, Study of the interaction between a new Schiff-base complex and bovine serum albumin by fluorescence spectroscopy, *Spectrochim. Acta Mol. Biomol. Spectrosc.* 77 (2) (2010) 430–436.